Trapping water monolayers with graphene allows AFM imaging

Layers of water molecules are present on all hydrophilic surfaces, yet studying these dynamic structures at room temperature is problematic. Imaging them with scanning probe microscopy is usually hindered by the formation of a capillary meniscus between the tip and sample. K. Xu of Harvard University and P. Cao and J.R. Heath at the California Institute of Technology have managed to overcome this difficulty by trapping water adlayers on mica beneath a monolayer of graphene.

As reported in the September 3rd issue of *Science* (DOI: 10.1126/science.1192907; p. 1188), Xu and coworkers deposit a layer of graphene onto mica through mechanical exfoliation, and identify monolayer regions using spatially resolved Raman spectroscopy. Imaging the surface with an atomic force microscope (AFM) under ambient conditions reveals raised regions of graphene thought to be the result of water monolayers trapped beneath it. The height of these islands (corresponding to a layer of ice), and the strong influence of the humidity conditions on the trapped layers point to their identity as water molecules. The monolayer islands form polygonal shapes, with geometries which suggest an ice-like structure formed epitaxially on the mica.

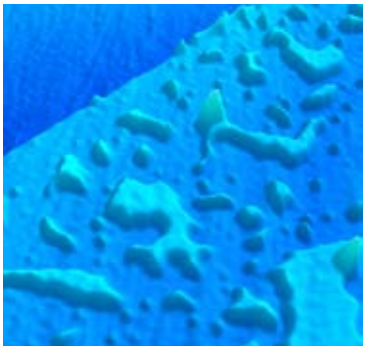

The atomic force micrograph shows monolayer islands of water trapped beneath a graphene sheet. More liquid-like water droplets are indicated by the higher peaks.

Imaging at varying relative humidity sheds further light on the mechanism of monolayer formations and their evolution at higher coverages. At low humidity (<2%), water islands could only be seen on mica with lots of surface defects. A tendency for the islands to connect defects demonstrates that defects play a role in nucleation of the monolayer. At higher humidity (~90%), complete monolayers were observed, as well as second layer islands, again often associated with surface defects. The height and geometry of these second layers were also in agreement with an ice-like model.

These results help elucidate a growth mechanism for water adlayers on mica that is remarkably similar to epitaxial growth in well-known inorganic systems. A complete monolayer is formed before the buildup of strain results in islands at higher coverages.

Tobias Lockwood

Nano Focus

Multishell nanoparticles created within a solid matrix

Particle inclusion in solid matrices is a common strategy used to tailor the properties of structural metallic alloys, such as strength or aging at elevated temperatures; however, it is a complicated story. Requirements for these particles that affect their interaction with dislocations and coarsening resistance are an often contradictory mix of stiffness, shearability, lattice parameter mismatch, diffusivities, and interfacial energies among other considerations. Earlier studies of solid-state precipitation within metallic alloys have focused on chemically homogenous nanoparticles. The ability to generate and tune more complex, chemically heterogeneous nanoparticle structures could lead to increased control over the macroscopic properties of important structural alloys. In a communication recently published in the August 16th issue of *Small* (DOI: 10.1002/smll.20100325; p. 1728) C. Monachon, D.C. Dunand, and D.N. Seidman of Northwestern University (Monachon now at EPFL, Switzerland) report a solid-state synthesis of nanoparticles with a core and two concentric shells within an aluminum-based alloy matrix. While this nanoparticle architecture has been achieved in solution-based syntheses, this work represents the first demonstration of multishell nanoparticles created within a solid matrix.

Their nanoparticles are created using a two-step aging protocol on an aluminum-based alloy

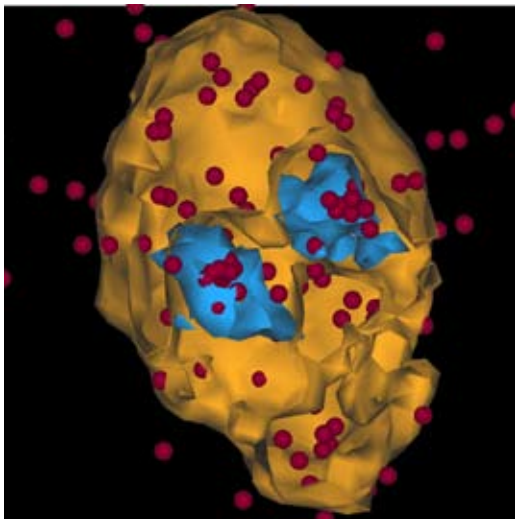

Atom-probe tomography reconstruction of a "double-yolk egg" nanoparticle containing two Yb-rich $Al_3(Li,Yb,Sc)$ cores, surrounded by their respective Sc-rich $Al_3(Li,Sc,Yb)$ first shells and a common δ'-Al_3Li second outer shell. Yb atoms are shown in red, Sc-rich regions in blue, and Li-rich regions in yellow. Image courtesy of David Seidman. Reproduced with permission from *Small* **6** (16) (2010) DOI: 10.1002/smll.20100325; p. 1728. © 2010 WILEY-VCH Verlag GmbH & Co.

https://doi.org/10.1557/mrs2010.719 Published online by Cambridge University Press

(Al-6.3Li-0.069Sc-0.018Yb, at.%) and characterized by dark field transmission electron microscopy and atom probe tomography (APT). The alloy is homogenized at 640°C followed by quenching in iced brine which generates large (1.5 μm) particles at grain boundaries containing Li, Sc, and Yb.

The first aging step, at 325°C, results in precipitation of Al_3X core–shell nanoparticles (where X can be Li, Sc, or Yb). The core is richer in Yb, and Sc is simultaneously enriched in the shell. The alloy is subsequently quenched to 170°C and aged, promoting the formation of a second shell around the particles composed of δ′-Al_3Li.

APT studies also revealed two populations of nanoparticles. The first is an abundant population of core–single-shell nanoparticles, with an average diameter of 2.2 nm ± 0.8 nm. The second particles are core–multishell nanoparticles with an average diameter of 12.2 nm ± 0.3 nm.

A representative particle has a core region of about 3.3 nm, a 1.8-nm thick (on average) first shell, and a 10-nm thick (on average) second shell. As an interesting case, one of these particles was actually a multicore–multishell particle containing two cores with single-shell encapsulated together in a δ′-Al_3Li second shell.

According to the researchers, this is a demonstration of the limitation of control over nanoscale features with this technique, but also an unexpected new architecture possible with this solid-state synthesis technique representing a minor but measureable subpopulation. Vickers microhardness tests show an increase in microhardness from 725 ± 10 MPa after the first aging step, when the core–single-shell nanoparticles are present, to 960 ± 20 MPa after the second aging, when core–multishell nanoparticles are also present providing evidence that the more complex multishell architecture has an advantage over core–single-shell particles.

The researchers said that this solid-state synthesis technique should be generally applicable to a range of alloys. Key considerations are (1) choice of alloying elements, relative diffusivities, and solubilities, and (2) choice of aging temperatures, which significantly affects the ability to segregate the elements and form multiple shells.

Continued tuning and understanding of the effects of complex multishell (and multicore) nanoparticles within solid matrices will allow even greater flexibility in tailoring alloy mechanical properties.

Alia P. Schoen

Nano Focus

Electrified nanostructures enable low-cost water sterilization

Waterborne bacterial diseases represent a major global problem killing over two million people worldwide annually, mostly children in developing countries. Conventional filters used to prevent such diseases are made from membranes but clogging of such devices is a common problem. A new strategy for deactivating bacteria by incorporating antibacterial silver nanowires (Ag NWs) in a carbon nanotube (CNT)-coated cotton fiber matrix has now been demonstrated. The material is mechanically robust, electrically conductive, and uses a very small amount of current to inactivate bacteria, while the open structure allows for high volume water filtration. The work led by Y. Cui and S. Heilshorn at Stanford University was published in the September 8th issue of *Nano Letters* (DOI: 10.1021/nl101944e; p. 3628).

Three components with different functionalities spanning three length scales formed the filter: (1) inexpensive cotton cloth formed the structural backbone, (2) Ag NWs (diameters of 40–100 nm, up to 10 μm long) with antibacterial properties formed a secondary mesh, and (3) carbon nanotubes formed a conductive coating on the cotton fibers. The final material (Ag NW/CNT cotton) was shaped into a cylindrical filter (4 mm diameter, 2.5 mm length) and placed in the stem of a glass funnel. Water was poured through the funnel at a typical flow rate of 1 L/h, with an applied low voltage of up to ±20 V. *Escherichia coli* was used as the representative bacterial species.

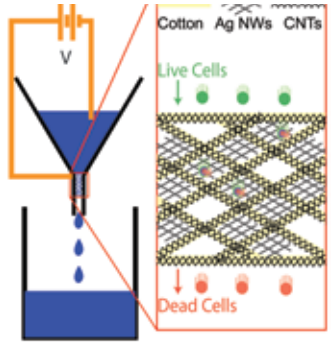

Schematic of the filtration device showing the three components used and the testing technique used for evaluation. NWs is nanowires and CNT is carbon nanotube. Reproduced with permission from *Nano Lett*. **10** (9) (2010) DOI: 10.1021/nl101944e; p. 3628. © 2010 American Chemical Society.

When no bias voltage was applied, neither the Ag NW/CNT cotton filter nor CNT-only cotton eliminated bacteria. On the other hand, the Ag NW/CNT cotton inactivated 89% of bacteria at −20 V and 77% at +20 V applied voltage, much higher than the CNT-only cotton. The Ag NW/CNT cotton device consumed 60 mW power, compared to 250 mW consumed by an equivalent ultrafiltration membrane. The Ag NW/CNT cotton device was effective in deactivating bacteria over a range of bacterial concentrations with modest power consumption. Three stages of this process were used in series to attain inactivation efficiencies of over 98%.

The material developed could form the basis of inexpensive point-of-use water filters for deactivating water-based microorganisms with high volume throughput. Such filters are ideal for use in developing countries due to the low cost of the filter and the modest electricity requirements.

Gopal R. Rao

https://doi.org/10.1557/mrs2010.719 Published online by Cambridge University Press